Inhalation Toxicology, 12:491–510, 2000

0895–8378/00 $12.00 + .00

A LUNG MODEL DESCRIBING UPTAKE OF ORGANIC SOLVENTS AND ROLES OF MUCOSAL BLOOD FLOW AND METABOLISM IN THE BRONCHIOLES

Shinji Kumagai, Ichiro Matsunaga

Department of Occupational Health, Osaka Prefectural Institute of Public Health, Osaka, Japan

A simple lung model (mucosal blood flow and metabolism model, MBM model) was developed to describe the uptake of organic solvents and investigate the role of mucosal blood flow and metabolism. The model separates the lung into four compartments, the peripheral bronchial tract (gas phase), the mucus layer lining the wall surface of the tract, the alveolar space (gas phase), and the alveolar blood. Solvent molecules are absorbed in the mucus layer during inhalation and released during exhalation. The deposited solvent diffuses radially into the mucosal tissue of the respiratory tract and transfers to the mucosal blood flow. To describe this behavior, a hypothetical mucosal blood flow throughout the mucus layer was used. The solvent in the mucosal tissue may be also metabolized, and a hypothetical metabolism in the mucus layer was used. The rate of the hypothetical mucosal blood flow was determined to be 5.2 ml/min based on the best fitting of previously obtained data for seven polar organic solvents. The MBM model predicts that as the blood–air partition coefficient (λ_B) increases from 0.1 to 20, the relative end-exhalation (E_{end}) will decrease from 0.89 to 0.07, and as λ_B increases to 500, E_{end} will increase to 0.33. After λ_B = 500, E_{end} is predicted to decrease again, and at λ_B = 10000, E_{end} is 0.09. The model also predicts that as λ_B increases from 0.1 to 10, the relative uptake (U) increases from 0.08 to 0.61, and as λ_B increases to 150, U decreases to 0.50. After λ_B = 150, U increases again, and at λ_B = 10,000, U is 0.8. The predictions show good agreement with values observed in human experimental studies. The MBM model predicts that uptake by the mucosal blood (U_{Al}) would be equal to uptake by the alveolar blood (U_{Mu}) at λ_B of 1000 and U_{Al} is more than 90% of total uptake at λ_B > 10,000. The model also shows that U is significantly increased by the mucosal metabolism at λ_B between 50 and 5000. Especially, U in the case of CL_{Mu} = 100 ml/min is higher by 0.3 than that in the nonmucosal metabolism.

Physiologically based pharmacokinetic (PBPK) models have been developed to simulate uptake, distribution, metabolism, and elimination of chemicals (Fiserova-Bergerova et al., 1974; Ramsey & Anderson, 1984; Droz et al., 1989; Fernandez et al., 1977; Koizumi, 1989; Johanson, 1986). Although such models require a substantial amount of information including ventilation rate, cardiac output, metabolic rate, and tissue–blood partition coefficients, they allow estimation of the concentrations of a

Received 28 July 1999; sent for revision 27 August 1999; revision returned 25 October 1999; accepted 29 October 1999.

Address correspondence to Shinji Kumagai, Department of Occupational Health, Osaka Prefectural Institute of Public Health, 1-3-69, Nakamichi, Higashinari-ku, Osaka, 537 Japan. E-mail: kumagai@iph.pref.osaka.jp

chemical in blood, tissue groups, exhaled air, and urine by inputting a scenario of airborne exposure.

In commonly used PBPK models, the conducting airway of the respiratory tract is considered to be an inert tube used for transport of the chemicals from the nose/mouth to the alveolar region, and the actual exchange with the body takes place in the alveolar region. Such models can be used for describing the lung kinetics of slightly water–soluble chemicals, such as toluene and trichloroethylene. However, these models are not applicable to highly water-soluble or blood-soluble solvents, such as ketones and alcohols, because the mucus layer lining the wall of the respiratory tract absorbs the solvents during inhalation and releases them during exhalation. This is called "washin–washout behavior." Johanson (1991) and Kumagai and Matsunaga (1995) proposed lung models that included the mucus layer as a compartment and could describe this washin–washout behavior. These models could be applied to solvents with blood–air partition coefficients (λ_B) of 100 to 500, such as acetone (Johanson, 1991; Kumagai & Matsunaga, 1995). However, for solvents with λ_B of about 10,000, such as glycol ethers, the estimated relative respiratory uptake was about 0.4 (Johanson, 1991) while the observed values were about 0.8 (Kumagai et al., 1999; Kezic et al., 1997). This discrepancy can be explained by the following behavior. The solvent molecules deposited in the mucus layer diffuse radially into the mucosal tissue of the respiratory tract and transfer to the mucosal blood flow. With higher λ_B, the effect of the mucosal blood flow on solvent uptake must become larger, because the solvent concentration in the mucosal blood increases.

Our previous study (Kumagai et al., 1999) found that relative respiratory uptakes for methyl acetate and ethyl acetate were higher by 0.07–0.15 than that for methyl *iso*-butyl ketone and methyl propyl ketone, though the λ_B values were nearly equal among these solvents. This is probably due to the mucosal metabolism in the respiratory tract, because their metabolites, methyl alcohol and ethyl alcohol, were detected in the exhaled air at the first minute (Kumagai et al., 1999).

In this study, we developed a simple lung model that can describe the removal of an organic solvent by the mucosal blood flow and metabolism, and then used it to investigate the role of mucosal blood flow and metabolism.

METHODS

Mucosal Blood Flow and Metabolism Model

Model Structure Figure 1 shows the mucosal blood flow and metabolism (MBM) model in which the deposition of solvent molecules into the mucus layer and their removal by the mucosal blood flow and metabolism

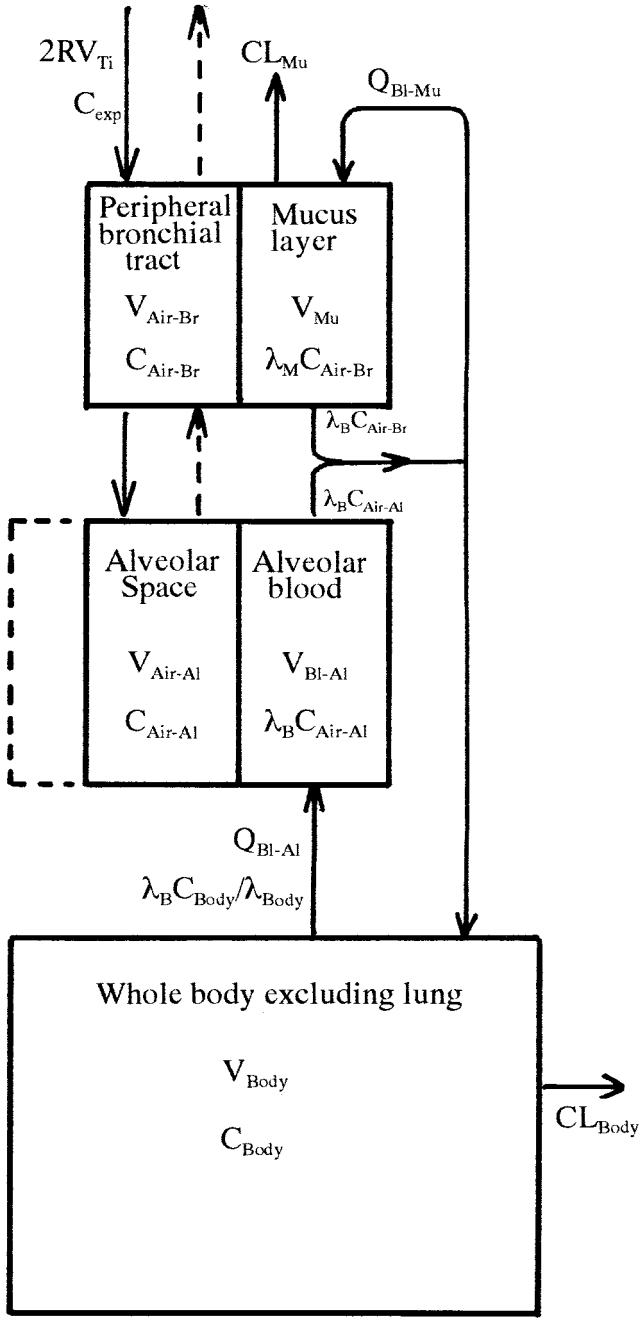

FIGURE 1. Diagram of a lung model considering mucosal blood flow and metabolism in bronchial tract (MBM model). Definitions of abbreviations are shown in Table 1.

are taken into account. In this model, the lung consists of four compartments; the peripheral bronchial tract (gas phase), the mucus layer lining the wall surface of the tract, the alveolar space (gas phase), and the alveolar blood. This model does not include the nasal cavity, because human experimental uptake data used for best fitting to the model were obtained under mouth respiration, not nose respiration. According to Johanson (1991), less than 10% of the solvent molecules are predicted to have wall contact in regions of the trachea to the subsegmental. Thus, the deposition of solvent in the mucus layer can be negligible, and the proximal tracheobronchial tract is assumed to be respiratory dead space. In contrast, the value is about 70% in the small bronchi, and practically 100% in the bronchioles and terminal bronchioles (Johanson, 1991), so that the solvent concentration in the peripheral bronchial tract ($C_{\text{Air-Br}}$) can be assumed to equilibrate with that in the mucus layer of the wall surface. It is also assumed that solvent concentration in the alveolar space ($C_{\text{Air-Al}}$) equilibrates with that in the alveolar blood. The volumes of the respiratory dead space (proximal tracheobronchial tract), peripheral bronchial tract, mucus layer, alveolar space, and alveolar blood are denoted as V_{Dead}, $V_{\text{Air-Br}}$, V_{Mu}, $V_{\text{Air-Al}}$, and $V_{\text{Bl-Al}}$, respectively.

In the MBM model, breathing is treated as a cyclic pattern of inhalation and exhalation. The effective tidal volume and respiratory rate are denoted as V_{Ti} and R, respectively. Consequently, the flow rate at inhalation or exhalation is $2RV_{\text{Ti}}$. $V_{\text{Air-Al}}$ is a function of time, expressed as $V_{\text{FR}} + V_{\text{Ti}}t/T$ during inhalation and $V_{\text{FR}} + V_{\text{Ti}}(2T - t)/T$ during exhalation, where V_{FR} is a functional residual capacity, T is a period of inhalation or exhalation (= $1/2R$), and t is the time after the start of inhalation. Alveolar blood flow is treated as a continuous process and the flow rate is denoted as $Q_{\text{Bl-Al}}$.

Solvent molecules deposited in the mucus layer diffuse radially into the mucosal tissue of the wall surface of the respiratory tract and transfer to the mucosal blood flow (Onorato et al., 1994). In the MBM model, for simplification, the two behaviors of diffusion and transfer are described as removal by a hypothetical blood flow throughout the mucus layer, though in reality, blood vessels form the submucosal plexus in the deeper portion of the mucosa (Deffebach et al., 1987). Thus, the hypothetical blood flow can be regarded as an effective mucosal blood flow on the mucus layer, so that the flow rate (denoted by $Q_{\text{Bl-Mu}}$) may be smaller than the total flow rate of the mucosal blood flow. The venous blood from the proximal tracheobronchial tract drains to the systemic circulation through the bronchial veins, while the major portion of the intrapulmonary bronchial venous blood drains into the pulmonary circulation through the bronchopulmonary anastomoses (Figure 1) (Deffebach et al., 1987).

Solvent molecules that diffuse into the mucosal tissue are removed by the metabolism for some solvents (e.g., esters) (Kumagai et al., 1999). In the MBM model, the two behaviors of diffusion and removal are also described as removal by a hypothetical metabolism in the mucus layer. Thus, the mucosal metabolic clearance in the MBM model (denoted by CL_{Mu}) may be smaller than the true value in the mucosal tissue.

In this study, for simplification, the whole body excluding the lung is treated as one compartment. The volume and solvent concentration of the whole body are denoted as V_{Body} and C_{Body}. The total clearance (excretion and metabolism of the solvent) in the whole body is denoted as CL_{Body}.

The kinetic behavior of a solvent can be described by the following simultaneous differential equations (detailed in the Appendix). Definitions of abbreviations are shown in Table 1.

During inhalation, there are three equations.

Peripheral bronchial region:

$$\frac{dC_{AirBr}}{dt} = -\frac{1}{(V_{AirBr} + \lambda_M V_{Mu})}\{[2RV_{Ti} + \lambda_B Q_{BlMu} + \lambda_M CL_{Mu} - \lambda_B Q_{BlMu} Q_{BlMu}/(Q_{BlAl} + Q_{BlMu})]C_{AirBr} - [\lambda_B Q_{BlMu} Q_{BlAl}/(Q_{BlAl} + Q_{BlMu})]C_{AirAl} - 2RV_{Ti}C_{exp}\} \quad (1)$$

TABLE 1. Parameter definition and values used in MBM model

Concentration		
C_{exp}	Exposure concentration	
$C_{Air\text{-}Br}$	Solvent concentration in peripheral bronchial tract	
$C_{Air\text{-}Al}$	Solvent concentration in the alveolar space	
C_{Body}	Solvent concentration in whole body	
Partition coefficient		
λ_B	Blood–air partition coefficient	
λ_M	Mucus–air partition coefficient	
λ_{Body}	Body–air partition coefficient	
Volume		
V_{Dead}	Respiratory dead space	60 ml
$V_{Air\text{-}Br}$	Peripheral bronchial tract	90 ml
V_{Mu}	Mucus layer	2.5 ml
$V_{Air\text{-}Al}$	Alveolar space during inhalation	$V_{FR} + V_{Ti}t/T$
	Alveolar space during exhalation	$V_{FR} + V_{Ti}(2T - t)/T$
$V_{Bl\text{-}Al}$	Alveolar blood	1000 ml
V_{Body}	Whole body excluding lung	65,000 ml
Respiration		
V_{Ti}	Effective tidal volume	440 ml
V_{FR}	Functional residual capacity	2700 ml
R	Respiratory rate	14 min^{-1}
T	$1/2R$	$^1/_{28}$ min
t	Time after start of inhalation	
Blood flow		
$Q_{Bl\text{-}Al}$	Alveolar blood flow	6000 ml/min
$Q_{Bl\text{-}Mu}$	Mucosal blood flow	5.2 ml/min
Clearance		
CL_{Mu}	Mucosal metabolism	0, 1, 5, 20, 100 ml/min
CL_{Body}	Whole-body metabolism and excretion	0, ∞ ml/min

Alveolar region:

$$\frac{dC_{AirAl}}{dt} = \frac{1}{V_{FR} + V_{Ti}t/T + \lambda_B V_{BlAl}} \{2RV_{Ti}C_{AirBr} - (\lambda_B Q_{BlAl} + 2RV_{Ti})C_{AirAl} + \lambda_B Q_{BlAl} C_{Body}/\lambda_{Body}\} \quad (2)$$

Body:

$$\frac{dC_{Body}}{dt} = \frac{1}{V_{Body}} \{[\lambda_B Q_{BlAl} Q_{BlAl}/(Q_{BlAl} + Q_{BlMu})]C_{AirAl} + [\lambda_B Q_{BlMu} Q_{BlAl}/(Q_{BlAl} + Q_{BlMu})]C_{AirBr} - (\lambda_B Q_{BlAl}/\lambda_{Body} + CL_{Body})C_{Body}\} \quad (3)$$

During exhalation there are also three equations.

Peripheral bronchial region:

$$\frac{dC_{AirBr}}{dt} = -\frac{1}{(V_{AirBr} + \lambda_M V_{Mu})} \{[2RV_{Ti} + \lambda_B Q_{BlMu} + \lambda_M CL_{Mu} - \lambda_B Q_{BlMu} Q_{BlMu}/(Q_{BlAl} + Q_{BlMu})]C_{AirBr} - [2RV_{Ti} + \lambda_B Q_{BlMu} Q_{BlAl}/(Q_{BlAl} + Q_{BlMu})]C_{AirAl}\} \quad (4)$$

Alveolar region:

$$\frac{dC_{AirAl}}{dt} = \frac{1}{V_{FR} + V_{Ti}(2T - t)/T + \lambda_B V_{BlAl}} (-\lambda_B Q_{BlAl} C_{AirAl} + \lambda_B Q_{BlAl} C_{Body}/\lambda_{Body}) \quad (5)$$

Body: The equation is the same as during inhalation.

Parameter Values (Table 1) As stated earlier, less than 10% of the solvent molecules are predicted to have wall contact in the subsegmental bronchi and upper regions (54 ml), about 70% in the small bronchi (14 ml), and practically 100% in the bronchioles and terminal bronchioles (81 ml) (Johanson, 1991). Thus, V_{Dead} and $V_{Air\text{-}Br}$ are 60 ml (≈ 54 + 14 × 0.3) and 90 ml (≈ 81 + 14 × 0.7), respectively, in the MBM model. The true tidal volume is about 500 ml (Stahl, 1967), but V_{Ti} is 440 ml, because the proximal tracheobronchial tract is the respiratory dead space. V_{FR} is 2.7 L and R is 14 min^{-1} for normal breathing (Stahl, 1967). The surface area of the peripheral bronchial tract (from the small bronchi to the terminal bronchioles) is about 5000 cm^2 (Johanson, 1991). Little data are available on the thickness of the mucus layer; however, a value of 5–10 μm has been suggested (Johanson, 1991). In this study, the thickness is assumed

to be 5 μm, so that V_{Mu} is 2.5 ml. $V_{Bl\text{-}Al}$ and $Q_{Bl\text{-}Al}$ are 1 L and 6 L/min, respectively (Droz et al., 1989). V_{Body} is 65 L for a standard male.

As stated earlier, $Q_{Bl\text{-}Mu}$ in the MBM model is not an anatomical parameter but an effective mucosal blood flow on the mucus layer of the wall surface. In our previous study (Kumagai et al., 1999), solvent concentrations in the end-exhaled air (C_{end}) and in the mixed exhaled air (C_{mix}) were determined during 10-min exposure of 7 polar organic solvents, methyl *iso*-butyl ketone, methyl propyl ketone, acetone, *iso*-propyl alcohol, methyl alcohol, ethylene glycol monobutyl ether, and propylene glycol monomethyl ether (Table 2), where C_{end} is an instantaneous solvent concentration in exhaled air at the end of exhalation, and C_{mix} is a mean solvent concentration in air exhaled during the whole exhalation. In our experiment (Kumagai et al., 1999), the solvent concentration in exhaled air was measured by continuously introducing a part of exhaled air to a flame ionization detector and C_{end} was determined to be the solvent concentration at the end of exhalation. Also, exhaled air was collected in a Tedlar bag during the whole exhalation and C_{mix} was determined by a gas chromatograph. Thus, the C_{end} value was obtained during exposure under the normal breath pattern (without lung washing with breath of clean air). It should be noted that the C_{end} value measured during exposure differs greatly from that after exposure (with one or more breaths of clean air prior to sampling), as shown by Petreas et al. (1995). From the observed values of C_{end} and C_{mix}, the relative end-exhalation (E_{end}) and relative respiratory uptake (U) were calculated as follows:

$$E_{end} = C_{end}/C_{exp}$$

$$U = 1 - C_{mix}/C_{exp}$$

where C_{exp} is exposure concentration.

TABLE 2. Blood–air partition coefficient (λ_B), relative end-exhalation (E_{end}), and relative respiratory uptake (U) in seven organic solvents

Solvent	λ_B	E_{end}[d]	U[d]
Methyl *iso*-butyl ketone	90[a]	0.20	0.53
Methyl propyl ketone	150[a]	0.27	0.54
Acetone	245[a]	0.30	0.54
iso-Propyl alcohol	848[b]	0.28	0.61
Methyl alcohol	2590[b]	0.26	0.62
Ethylene glycol monobutyl ether	7970[c]	0.07	0.81
Propylene glycol monomethyl ether	12,380[c]	0.12	0.82

[a]Sato and Nakajima (1979a).
[b]Kaneko et al. (1994).
[c]Johanson and Dynesius (1988).
[d]Kumagai et al. (1999).

Using these observed values of E_{end} and U, the $Q_{Bl\text{-}Mu}$ value was determined by increasing from 0.1 ml/min in 0.1-ml/min increments until the best fit of the calculated values (by the following computer calculation) to the observed ones was obtained as assessed by least squares $[\Sigma(E_{end(E,i)} - E_{end(O,i)})^2 + \Sigma(U_{(E,i)} - U_{(O,i)})^2$, where $E_{end(E,i)}$ and $E_{end(O,i)}$ were the estimated and observed values of E_{end}, respectively, for solvent i, and $U_{(E,i)}$ and $U_{(O,i)}$ were the estimated and observed values of U, respectively].

In the computer calculation for the best fit, the whole-body compartment was ignored, because vapor pressure in the venous blood leaving the whole body during the first 10 min can be considered negligible due to the high λ_B value of the 7 organic solvents. The value of λ_M was assumed to be equal to λ_B. CL_{Mu} was assumed to be 0, because the metabolism of the seven solvents in the mucosal tissue was considered to be low.

Model Prediction for Organic Solvents Without the Mucosal Metabolism For organic solvents without the mucosal metabolism, E_{end} and U at 10 min after the start of exposure were predicted against λ_B of 0.1 to 50,000, using the following computer simulation. First, $CL_{Mu} = 0$ and $\lambda_M = \lambda_{Body} = \lambda_B$. Two cases were considered for the total solvent clearance in the whole body. One was a very high-clearance case, so that $CL_{Body} = \infty$ ($C_{Body} = 0$). Another was a very low-clearance case, so that $CL_{Body} = 0$. Considering the cyclic breathing pattern [Eqs. (1) and (2) during inhalation, Eqs. (4) and (5) during exhalation], E_{end} at 10 min after the start of exposure was calculated by the Runge–Kutta–Gill method with a software package developed by Yamaoka (1984). This predicted value of E_{end} was the relative end-exhalation during exposure under the normal breath pattern (without lung washing by breath of clean air and without breath holding). Simultaneously, U, the relative uptake by the alveolar blood (U_{Al}) and the relative uptake by the mucosal blood in the respiratory tract (U_{Mu}) were calculated as follows:

$$U = 1 - \int 2RV_{Ti}C_{Air\text{-}Br}\, dt/(V_{Ti} + V_{Dead})C_{exp}$$

where the integration was taken during 1 exhalation at 10 min after the start of exposure, and

$$U_{Al} = \int Q_{Bl\text{-}Al}\, \lambda_B\, C_{Air\text{-}Al}\, dt/(V_{Ti} + V_{Dead})C_{exp}$$

$$U_{Mu} = \int Q_{Bl\text{-}Mu}\, \lambda_B\, C_{Air\text{-}Br}\, dt/(V_{Ti} + V_{Dead})\, C_{exp}$$

where the integrations were taken during one circle of inhalation and exhalation at 10 min after the start of exposure.

Model Prediction for Organic Solvents With the Mucosal Metabolism For organic solvents with the mucosal metabolism, E_{end} and U at 10 min after the start of exposure were predicted using similar computer simulation. CL_{Mu} was selected as 1, 5, 20, or 100 ml/min.

Modified Perfusion Ventilation Model (PV′ Model) and Mucus Layer Model (ML Model)

For comparison, E_{end} and U were estimated by the PV′ model in which the whole conducting airway (from nose/mouth to terminal bronchioles) is treated as a respiratory dead space (V_{Mu} = 0 ml, $Q_{Bl\text{-}Mu}$ = 0 ml/min, CL_{Mu} = 0 ml/min). This is the same as a commonly used PV model except for the breathing pattern (cyclic vs. continuous). Another comparison was done using the ML model in which the mucus layer is included, but the mucosal blood flow is not considered (V_{Mu} = 2.5 ml, $Q_{Bl\text{-}Mu}$ = 0 ml/min, CL_{Mu} = 0 ml/min).

Comparison With E_{end} and U Values Reported by Other Investigators

The predicted E_{end} and U were compared with the observed values in human experimental studies selected according to the following criteria (criterion 1 for E_{end}, 2 or 3 for U):

1. The E_{end} value was measured at 0 to 10 min after the start of exposure at rest condition without lung washing by breathing of clean air and without breath holding, and the value was reported in the text, table, or figure.
2. The U value was measured at 0 to 10 min after the start of exposure (including mean value during the first 20 min) at rest condition and the value was reported in the text, table, or figure.
3. The U value was measured at 0 to 10 min after the start of exposure under rest condition. Although the value was not reported, the mean value over the whole exposure duration was reported, and it was noted that the U value was constant over the period.

RESULTS

Selected Value of $Q_{Bl\text{-}Mu}$

By the best fitting to our previous data for the seven organic solvents, $Q_{Bl\text{-}Mu}$ was determined to be 5.2 ml/min. The predicted values deviated from the observed values, on the average, by 0.024 for E_{end} and 0.034 for U.

MBM Model Prediction

Figure 2 shows the predicted relationship between λ_B and E_{end} from the computer simulation. For $CL_{Body} = \infty$, as λ_B increased from 0.1 to 20, E_{end} was predicted to decrease from 0.89 to 0.07, and as λ_B increased to 500, E_{end} was predicted to increase to 0.33. After λ_B = 500, E_{end} was predicted to decrease again, and at λ_B = 10,000, E_{end} was 0.09. E_{end} for CL_{Body} = 0 was predicted to be higher by 0.05–0.17 than E_{end} for $CL_{Body} = \infty$ when $\lambda_B < 10$, but these values were close to each other when $\lambda_B > 50$. Figure 2 also shows the observed values of E_{end} in studies by Kumagai et al. (1999),

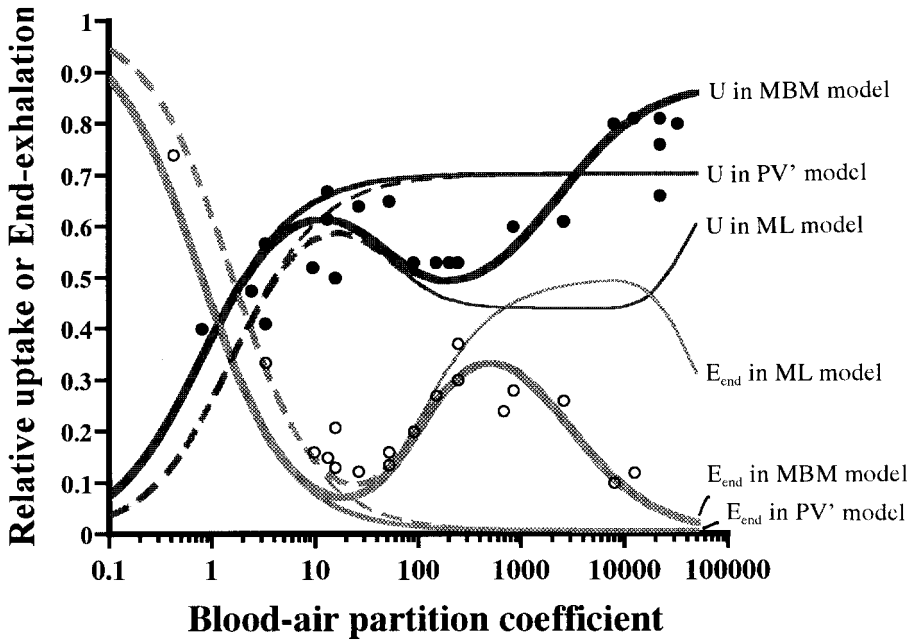

FIGURE 2. Predicted relationships between partition coefficient and relative end-exhalation (E_{end}) and between partition coefficient and relative uptake (U) at 10 min after start of exposure, and observed relationships in human experimental studies. Solid line: $CL_{Body} = \infty$. Broken line: $CL_{Body} = 0$. Open circles: observed values of E_{end} for desflurane (Jones et al., 1990) ($\lambda_B = 0.42$; Jones et al., 1990), 1,1,1-trichloroethane (Astrand et al., 1973) (3.3; Sato & Nakajima, 1979b), dichloromethane (Astrand et al., 1975) (9.7; Sato & Nakajima, 1979b), tetrachloroethylene (Fernandez et al., 1976) (13; Sato & Nakajima, 1979b), toluene (Carlsson, 1982; Dossing et al., 1984) (16; Sato & Nakajima, 1979a), xylene (Astrand et al., 1978) (26; Sato & Nakajima, 1979a), styrene (Pezzagno et al., 1985; Astrand et al., 1974) (52; Sato & Nakajima, 1979a), methyl *iso*-butyl ketone (Kumagai et al., 1999) (90; Sato & Nakajima, 1979a), methyl propyl ketone (Kumagai et al., 1999) (150; Sato & Nakajima, 1979a), acetone (Kumagai et al., 1999; Wigaeus et al., 1981) (245; Sato & Nakajima, 1979a), butanol (Astrand et al., 1976) (677; Kaneko et al., 1994), *iso*-propyl alcohol (Kumagai et al., 1999) (848; Kaneko et al., 1994), methanol (Kumagai et al., 1999) (2590; Kaneko et al., 1994), ethylene glycol monobutyl ether (Kumagai et al., 1999) (7970; Johanson & Dynesius, 1988), propylene glycol monomethyl ether (Kumagai et al., 1999) (12,400; Johanson & Dynesius, 1988). Closed circles: observed values of U for hexane (van Engelen et al., 1997) (0.8; Perbellini et al., 1985), carbon disulfide (Rosier et al., 1987) (2.4; McKee, 1941), 1,1,1-trichloroethane (Monster, 1979; Pezzagno et al., 1988), trichloroethylene (Monster, 1979) (9.5; Sato & Nakajima, 1979b), tetrachloroethylene (Monster, 1979; Pezzagno et al., 1988), toluene (Pezzagno et al., 1988), xylene (Pezzagno et al., 1988), styrene (Pezzagno et al., 1988), methyl *iso*-butyl ketone (Kumagai et al., 1999), methyl propyl ketone (Kumagai et al., 1999), methyl ethyl ketone (Liira et al., 1988) (202; Sato & Nakajima, 1979a), acetone (Kumagai et al., 1999; Pezzagno et al., 1988), *iso*-propyl alcohol (Kumagai et al., 1999), methanol (Kumagai et al., 1999), ethylene glycol monobutyl ether (Kumagai et al., 1999), propylene glycol monomethyl ether (Kumagai et al., 1999), ethylene glycol monoethyl ether (Kezic et al., 1997; Groeseneken et al., 1986, 1989) (22,100; Johanson & Dynesius, 1988), ethylene glycol monomethyl ether (Kezic et al., 1997) (32,800; Johanson & Dynesius, 1988).

Jones et al. (1990), Astrand et al. (1973, 1974, 1975, 1976, 1978), Fernandez et al. (1976), Carlsson (1982), Dossing et al. (1984), Pezzagno et al. (1985), and Wigaeus et al. (1981), selected according to the criteria given earlier. These values agree well with the model prediction, though the 3 values deviated by more than 0.05.

The predicted relationship between λ_B and U is shown in Figure 2. For $CL_{Body} = \infty$, as λ_B increased from 0.1 to 10, U was predicted to increase from 0.08 to 0.61, and as λ_B increased to 200, U was predicted to decrease to 0.50. After $\lambda_B = 150$, U increased again, and at $\lambda_B = 10{,}000$, U was 0.80. U for $CL_{Body} = 0$ was predicted to be lower by 0.05–0.12 than U for $CL_{Body} = \infty$ when $\lambda_B < 7$, but these values were close to each other when $\lambda_B > 40$. Figure 2 also shows the observed values of U in studies by Kumagai et al. (1999), Kezic et al. (1997), van Engelen et al. (1997), Rosier et al. (1987), Monster (1979), Pezzagno et al. (1988), Liira et al. (1988), Groeseneken et al. (1986, 1989), selected according to the criteria given earlier. These values showed good agreement with the model prediction, though 5 values deviated by more than 0.05.

PV′ Model and ML Model Predictions

Figure 2 also shows the relationships between λ_B and E_{end} predicted by the PV′ and ML models. At $\lambda_B = 0.1$ to 10, the predictions by the 2 models were very close to that by the MBM model. In the PV′ model, as λ_B increased from 20 to 50,000, E_{end} consistently decreased to 0. In the ML model, as λ_B increased from 20 to 10,000, E_{end} increased to 0.49, and it decreased after $\lambda_B = 10{,}000$. These behaviors differed greatly from that in the MBM model. The observed E_{end} values for ketones, alcohols, and glycol ethers deviated by more than 0.05 from the prediction by the PV′ model, and those for alcohols and glycol ethers deviated from the prediction by the ML model.

Figure 2 shows the relationships between λ_B and U predicted by the PV′ and ML models. At $\lambda_B = 0.1$ to 5, the predictions by the 2 models were very close to that by the MBM model. In the PV′ model, as λ_B increased from 10 to 50,000, U consistently increased to 0.70. In the ML model, as λ_B increased from 10 to 10,000, U decreased to 0.44, and it increased after $\lambda_B = 10{,}000$. These behaviors differed greatly from that in the MBM model. Comparison with the observed values suggested that the PV′ model did not fit for ketones, alcohols, and glycol ethers, and the ML model did not fit for alcohols and glycol ethers.

Washin–Washout Behavior

Figure 3 shows the predicted time courses of $C_{Air\text{-}Br}$ and $C_{Air\text{-}Al}$ during 1 cycle of inhalation and exhalation at 10 min after the start of exposure. The area between C_{exp} and $C_{Air\text{-}Br}$ corresponds to an amount of solvent deposited in the peripheral bronchial region during inhalation, so that it is a total of solvent absorbed in the mucus layer and solvent remaining in the peripheral bronchial tract. The area increased with λ_B increasing to 0.1 to 10,000, which suggested that washin behavior increased with λ_B. Area between $C_{Air\text{-}Br}$ and $C_{Air\text{-}Al}$ corresponds to an amount of solvent released from the peripheral bronchial region to the exhaled air during exhalation, so that it is a total of solvent released from the mucus layer and that from the peripheral bronchial tract. The area increased with λ_B increasing to 0.1 to 100 and decreased with λ_B inc

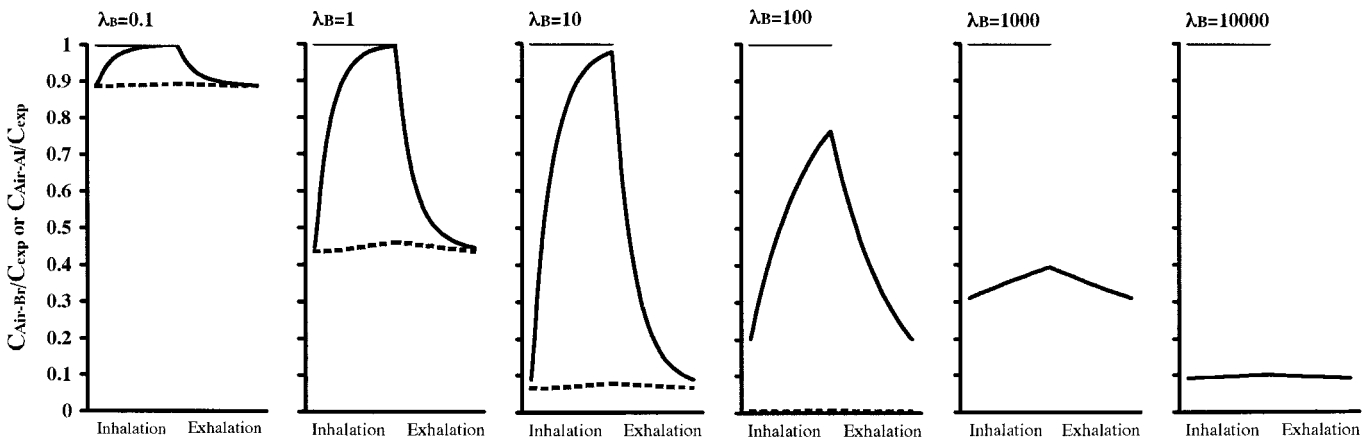

FIGURE 3. Time courses of solvent concentration in the peripheral bronchial tract ($C_{Air\text{-}Br}$) and that in the alveolar space ($C_{Air\text{-}Al}$). Thin solid line: C_{exp}. Thick solid line: $C_{Air\text{-}Br}$. Broken line: $C_{Air\text{-}Al}$.

10,000, which suggested that washout behavior occurred most highly at λ_B of about 100.

Uptakes by Alveolar and Mucosal Blood Flows

Figure 4 shows the predicted values of U_{Al} and U_{Mu} against λ_B. At $\lambda_B <$ 100, U_{Al} was predicted to be more than 90% of U. As λ_B increased from 100, U_{Al} decreased, while U_{Mu} increased. At λ_B = 1000, U_{Mu} was nearly equal to U_{Al}, and at $\lambda_B >$ 10,000, U_{Mu} was predicted to be more than 90% of U.

Effect of Mucosal Metabolism on Uptake

Figure 4 shows the predicted effect of the mucosal metabolism on uptake. The U value cannot be largely affected by the mucosal metabolism at $\lambda_B < 10$ or $\lambda_B >$ 20,000, but it was predicted to be significantly increased at λ_B 50 $< \lambda_B <$ 5000. Especially, U for CL_{Mu} = 100 ml/min was predicted to be higher by 0.3 than for CL_{Mu} = 0 ml/min.

DISCUSSION

We used our previous data of E_{end} and U values (Kumagai, 1999) to determine the value of $Q_{Bl\text{-}Mu}$ for the following reasons. First, these E_{end} and U values were obtained under the same experimental conditions for all solvents, thus making the values comparable. Second, these values were obtained within 10 min after the start of exposure and the λ_B values were 90 or more, which allow us to assume that solvent vapor pressure in the venous blood was negligible and enable us to observe the kinetic behavior of the solvent in the bronchial tract due to little effect of kinetics in the whole body on the exhaled air. Third, the bronchial metabolisms of ketones, alcohols, and glycol ethers are probably low, which allows the assumption of $CL_{Mu} = 0$.

Few data are available on the mucosal blood flow in the bronchial tract; however, the work of Onorato et al. (1994) suggests that the flow rate per unit surface area is about 8 μl/min/cm^2. Because the surface area of the peripheral bronchial tract is about 5000 cm^2 (Johanson, 1991), the total mucosal blood flow is about 40 ml/min for a first approximation. In the MBM model, $Q_{Bl\text{-}Mu}$ was determined to be 5.2 ml/min so that the best fit to the observed E_{end} and U was obtained for the 7 polar organic solvents. This discrepancy can be explained by the following consideration. Because the blood vessels form the submucosal plexus in the deeper portion of the mucosa (Deffebach et al., 1987), the solvent deposited in the mucus layer must diffuse into the deeper portion throughout the epithelium in order to transfer to the mucosal blood flow. In the MBM model, this behavior is described as the transfer to the hypothetical blood flow throughout the mucus layer. This must make the value of $Q_{Bl\text{-}Mul}$ smaller than the true mucosal blood flow. By similar consideration, the solvent

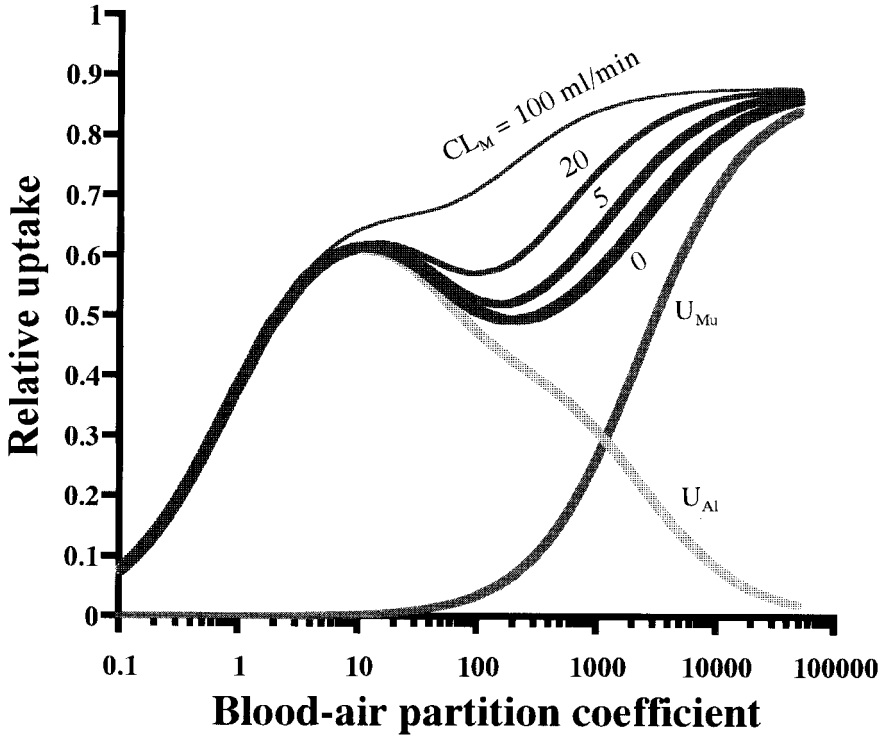

FIGURE 4. Relative uptake by the alveolar blood (U_{Al}) and by the mucosal blood in the respiratory tract (U_{Mu}), and effect of the mucosal metabolism on relative uptake.

concentration in the mucus layer of the MBM model may be different from that in the mucosal tissue of the peripheral bronchial tract. Consequently, the model cannot be used to investigate the effect of a chemical on the mucosal tissue. However, when the mucosal tissue is treated only as an uptake route into the body, the difference is not important.

Morris et al. (Morris & Cavanagh, 1986, 1987; Morris et al., 1986) and Aharonson et al. (1974) found that organic solvents including acetone, *iso*-propyl alcohol, and ethyl alcohol were taken into the body through the nasal wall tissue of animals. Dahl et al. (1991) quantitatively determined nasal uptake for 2,4-dimethylpentane, propyl ether, butanone, 1,3-dioxolane, and ethyl alcohol in dogs, and Gerde et al. (1991) proposed a model describing the nasal uptake. The model includes washin–washout behavior in the nasal cavity as well as removal of solvent from the nasal wall tissue by the nasal capillary blood flow, and it can appropriately predict the observed nasal uptake for the solvents with λ_B of 1 to 3000. As stated in the Methods section, our model does not include the nasal cavity, because the E_{end} and U values used for best fitting to the model were obtained under mouth respiration, not nose respiration. Frederick et al. (1998) proposed a physiologically based pharmacokinetic (PBPK) model in which

the deposition of solvent molecules into the nasal cavity and their removal by the nasal blood flow and metabolism are taken into account. They showed an important role of the human nasal cavity in uptake of water-soluble vapors, so that it may be necessary to modify our model by attaching a compartment of the nasal cavity. However, few experimental data are available on the solvent uptake from the human nasal cavity; it is important to confirm Frederick's result of the PBPK model by a human study.

As stated in the Methods section, C_{end} in this study is the solvent concentration in the end-exhaled air during exposure under normal breath pattern. The value differs greatly from the C_{end} value after exposure (with one or more breath of clean air prior to sampling), as shown by Petreas et al. (1995). For biological exposure monitoring, the end-exhaled air sample is taken in the uncontaminated area, which means the C_{end} value is that after exposure. Consequently, the predicted E_{end} in this study was not an index for biological monitoring, but was used to confirm that the model prediction was appropriate.

The MBM model could satisfactorily predict U and E_{end}, because the observed values well agreed with the prediction at λ_B = 0.4 to 30,000. The prediction showed that U increased with λ_B increasing from 0.1 to 10, but U decreased with λ_B increasing from 10 to 150. As shown in Figure 3, the washout behavior in the peripheral bronchial region occurred most highly at λ_B of about 100. This is why U decreased with λ_B increasing from 10 to 150. When λ_B increased from 150, U was predicted to increase again. As shown in Figure 4, U_{Mu} was predicted to increase rapidly after λ_B = 150, be nearly equal to U_{Al} at λ_B = 1000, and reach more than 90% of U at λ_B = 10,000. This suggests that the uptake by the mucosal blood flow causes the increase of U after λ_B = 150 and the blood flow plays an important role in the respiratory uptake of highly blood-soluble organic solvents.

When λ_B was less than 10, the predictions of U by the PV′ model and the ML model were almost the same as that by the MBM model. This is probably because the effect of washin–washout behavior on uptake was small. However, when λ_B was 100 to 1000, the predicted U values from the PV′ model were much higher than the observed ones, probably because the effect of washin–washout behavior on uptake became large and the PV′ model could not describe this behavior. When λ_B was 1000 or more, the predicted values from the ML model were much lower than the observed ones, probably because the effect of mucosal blood flow on uptake became large and the ML model could not describe the effect. In the ML model prediction, after λ_B = 10,000, E_{end} decreased and U increased. It is the reason that E_{end} and U did not reach steady-state levels in the peripheral bronchial tract at 10 min after the start of exposure due to the high λ_B. E_{end} and U were predicted to reached steady-state levels at 60 min and these values were 0.44 and 0.49, respectively, which is not agreement with the observed values.

Morris et al. (Morris & Cavanagh, 1987; Morris, 1990) found that some organic solvents were metabolized in the nasal cavity tissue in rat studies. Using their data, V_{max} in the respiratory mucosa of the nasal cavity can be calculated to be 0.067, 0.27, and 28 μg/min/cm^2, respectively, for xylene, *iso*-amyl alcohol, and ethyl acetate, and the Michaelis constant, K_m, to be 0.8, 1.5, and 720 μg/ml, respectively (Morris et al., 1993). Consequently, the intrinsic metabolic clearances are 0.084, 0.18, and 0.039 ml/min/cm^2 when solvent concentrations in the nasal cavity tissue are much lower than the K_m values. If the metabolic clearance in human bronchial tissue is the same level and the ratio of CL_{Mu} in the MBM model to the true metabolic clearance in the bronchial tissue is the same as the ratio of $Q_{Bl\text{-}Mu}$ to the true mucosal blood flow (5.2:40), then the CL_{Mu} values are 55, 120, and 25 ml/min. According to the MBM model prediction, the bronchial metabolic clearance for the three solvents must play an important role in the respiratory uptake. However, this is the case only when the solvent concentration in the bronchial tissue is much lower than the K_m value. Because the λ_B values of these solvents are 25 (Sato & Nakajima, 1997a) 381 (Kaneko et al., 1994), and 77 (Kaneko et al., 1994), respectively, for xylene, *iso*-amyl alcohol, and ethyl acetate, the solvent concentrations in the bronchial tract (gas phase) corresponding to the K_m values are 32, 3.9, and 9350 μg/l (7.4, 1.1, and 2600 ppm). This predicts that the bronchial metabolism of ethyl acetate does not reach saturation even at a very high exposure level, so that the metabolism extensively affects respiratory uptake. For xylene, when the exposure concentration is low, because the bronchial metabolism does not reach saturation, the metabolism highly affects the respiratory uptake. When the xylene concentration in the bronchial tract is 50 ppm, CL_{Mu} is 7.0 ml/min, which is larger than the $Q_{Bl\text{-}Mu}$ value, so that the role of metabolism is dominant. For *iso*-amyl alcohol, the bronchial metabolism reaches saturation at an even low exposure level, so that the CL_{Mu} must be much lower than 120 ml/min at a high exposure level. When the *iso*-amyl alcohol concentration in the bronchial tract is 50 ppm, CL_{Mu} is 2.5 ml/min, which is half of the $Q_{Bl\text{-}Mu}$ value, so that the role of metabolism is relatively small.

In the present study, the whole body was treated as one compartment and the body–blood partition coefficient was assumed to be 1. In reality, the tissue–blood partition coefficient differs among the tissue groups, and the blood flow to each tissue group also differs. The effects of these differences on the simulation result may not be high for short-term exposure (about 10 min). However, when the exposure duration increases, the effect must become large. This problem can be solved easily by attaching a conventional multicompartment PBPK model to the MBM model.

The MBM model can describe uptake of organic solvents, but the two behaviors of radial diffusion and blood transfer of the deposited solvent in mucus layer are described as removal by the hypothetical blood flow throughout the mucus layer. Because, in reality, blood vessels form the

submucosal plexus in the deeper portion of the mucosa (Deffebach et al., 1987), it is necessary to develop a diffusion-limited model for the tissue in order to describe the solvent behavior in the mucus layer and mucosal tissue in more detail.

APPENDIX

Peripheral Region

During inhalation, the following equation is set up based on mass balance in the peripheral region:

$$\frac{d(C_{AirBr}V_{AirBr} + \lambda_M C_{AirBr}V_{Mu})}{dt} = 2RV_{Ti}C_{exp} + \frac{\lambda_B Q_{BlMu}C_{AirBr} + \lambda_B Q_{BlAl}C_{AirAl}}{Q_{BlMu} + Q_{BlAl}} Q_{BlMu} - 2RV_{Ti}C_{AirBr} - \lambda_B Q_{BlMu}C_{AirBr} - \lambda_M CL_{Mu}C_{AirBr}$$

Consequently, Eq. (1) can be introduced. During exhalation, using $C_{Air\text{-}Al}$ instead of C_{exp} in the equation just shown, Eq. (4) can be introduced.

Alveolar Region

During inhalation, the following equation is set up based on mass balance in the alveolar region:

$$\frac{d(C_{AirAl}V_{AirAl} + \lambda_B C_{AirAl}V_{BlAl})}{dt} = 2RV_{Ti}C_{AirBr} + \lambda_B Q_{BlAl}C_{Body}/\lambda_{Body} - \lambda_B Q_{BlAl}C_{AirAl}$$

Because $V_{Air\text{-}Al} = V_{FR} + V_{Ti}t/T$, and $1/T = 2R$, the left side can be transformed to

$$(V_{FR} + V_{Ti}t/T + \lambda_B V_{BlAl})\frac{dC_{AirAl}}{dt} + 2RV_{Ti}C_{AirAl}$$

Consequently, Eq. (2) can be introduced. During exhalation,

$$\frac{d(C_{AirAl}V_{AirAl} + \lambda_B C_{AirAl}V_{BlAl})}{dt} = -2RV_{Ti}C_{AirAl} + \lambda_B Q_{BlAl}C_{Body}/\lambda_{Body} - \lambda_B Q_{BlAl}C_{AirAl}$$

Because $V_{Air\text{-}Al} = V_{FR} + V_{Ti}(2T - t)/T$, and $1/T = 2R$, the left side can be transformed to

$$[V_{FR} + V_{Ti}(2T - t)/T + \lambda_B V_{BlAl}]\frac{dC_{AirAl}}{dt} - 2RV_{Ti}C_{AirAl}$$

Consequently, Eq. (5) can be introduced.

Body

During inhalation and exhalation, the following equation is set up based on mass balance in the body:

$$\frac{dC_{Body}V_{Body}}{dt} = \frac{\lambda_B Q_{BlMu} C_{AirBr} + \lambda_B Q_{BlAl} C_{AirAl}}{Q_{BlMu} + Q_{BlAl}} Q_{BlAl} - \lambda_B Q_{BlAl} C_{Body}/\lambda_{Body} - CL_{Body} C_{Body}$$

Consequently, Eq. (3) can be introduced.

REFERENCES

Aharonson, E. F., Menkes, H., Gurtner, G., Swift, D. L., and Proctor, D. F. 1974. Effect of respiratory airflow rate on removal of soluble vapors by the nose. *J. Appl. Physiol.* 37:654–657.

Astrand, I., Kibom, A., Wahlberg, I., and Ovrum, P. 1973. Methylchloroform exposure. I. Concentration in alveolar air and blood at rest and during exercise. *Work Environ. Health* 10: 69–81.

Astrand, I., Kilbom, A., Ovrum, P., Wahlberg, I., and Vesterberg, O. 1974. Exposure to styrene. I. Concentration in alveolar air and blood at rest and during exercise and metabolism. *Scand. J. Work Environ. Health* 11:69–85.

Astrand, I., Ovrum, P., and Carlsson, A. 1975. Exposure to methylene chloride. I. Its concentration in alveolar air and blood at rest and during exercise and its metabolism. *Scand. J. Work Environ. Health* 1:78–94.

Astrand, I., Ovrum, P., and Linqvist, T. 1976. Exposure to butyl alcohol. Uptake and distribution in man. *Scand. J. Work Environ. Health* 3:165–175.

Astrand, I., Engstrom, J., and Ovrum, P. 1978. Exposure to xylene and ethylbenzene. I. Uptake, distribution and elimination in man. *Scand. J. Work Environ. Health* 4:185–194.

Carlsson, A. 1982. Exposure to toluene. Uptake, distribution and elimination in man. *Scand. J. Work Environ. Health* 8:43–55.

Dahl, A. R., Snipes, M. B., Gerde, P. 1991. Sites for uptake of inhaled vapors in Beagle dogs. *Toxicol. Appl. Pharmacol.* 109:263–275.

Deffebach, M. E., Charan, N. B., Lakshminarayan, S., and Butler, J. 1987. Thebronchial circulation. Small, but a vital attribute of the lung. *Am. Rev. Respir. Dis.* 135:463–481.

Dossing, M., Baelum, J., Hansen, S. H., and Lundqvist, G. R. 1984. Effect of ethanol, cimetidine and propranolol on toluene metabolism in man. *Int. Arch. Occup. Environ. Health* 54:309–315.

Droz, P. O., Wu, M. M., Gumgerland, W. G., and Berode, M. 1989. Variability in biological monitoring of solvent exposure. I. Development of a population physiological model. *Br. J. Ind. Med.* 46:447–460.

Fernandez, J., Guberan, E., and Caperos, J. 1976. Experimental human exposures to tetrachloroethylene vapor and elimination in breath after inhalation. *Am. Ind. Hyg. Assoc. J.* 37:143–150.

Fernandez, J. G., Droz, P. O., Humbert, B. E., and Caperos, J. R. 1977. Trichloroethylene exposure simulation of uptake, excretion, and metabolism using a mathematical model. *Br. J. Ind. Med.* 34:43–55.

Fiserova-Bergerova, V., Vlach, J., and Singhal, K. 1974. Simulation and prediction of uptake, distribution, and exhalation of organic solvents. *Br. J. Ind. Med.* 31:45–52.

Frederick, C. B., Bush, M. L., Lomax, L. G., Black, K. A., Finch, L., Kimbell, J. S., Morgan, K. T., Subramaniam, R. P., Morris, J. B., and Ultman, J. S. 1998. Application of a hybrid computational fluid dynamics and physiologically based inhalation model for interspecies dosimetry extrapolation of acidic vapors in the upper airway. *Toxicol. Appl. Pharmacol.* 152:211–231.

Gerde, P., and Dahl, A. R. 1991. A model for the uptake of inhaled vapors in the nose of the dog during cyclic breathing. *Toxicol. Appl. Pharmacol.* 109:276–288.

Groeseneken, D., Veulemans, H., and Masschelein, R. 1986. Respiratory uptake and elimination of

ethylene glycol monoethyl ether after experimental human exposure. *Br. J. Ind. Med.* 43:544–549.

Groeseneken, D., Veulemans, H., Masschelein, R., Vlem, E. V. 1989. Experimental human exposure to ethylene glycol monomethyl ether. *Int. Arch. Occup. Environ. Health* 61:243–247.

Johanson, G. 1986. Physiologically based pharmacokinetic modeling of inhaled 2-butoxyethanol in man. *Toxicol. Lett.* 34:23–31.

Johanson, G. 1991. Modeling of respiratory exchange of polar solvents. *Ann. Occup. Hyg.* 35:323–339.

Johanson, G., and Dynesius, B. 1988. Liquid/air partition coefficients of six commonly used glycol ethers. *Br. J. Ind. Med.* 45:561–564.

Jones, R. M., Cashman, J. N., Eger, E. I., Damask, M. C., and Johnson, B. H. 1990. Kinetics and potency of desflurane (I-653) in volunteers. *Anesth. Analg.* 70:3–7.

Kaneko, T., Wang, P. Y., and Sato, A. 1994. Partition coefficients of some acetate esters and alcohols in water, blood, olive oil, and rat tissues. *Occup. Environ. Med.* 51:68–72.

Kezic, S., Mahieu, K., Monster, A. C., and de Wolff, F. A. 1997. Dermal absorption of vaporous and liquid 2-methoxyethanol and 2-ethoxyethanol in volunteers. *Occup. Environ. Med.* 54:38–43.

Koizumi, A. 1989. Potential of physiologically based pharmacokinetics to amalgamate kinetic data of trichloroethylene and tetrachloroethylene obtained in rats and man. *Br. J. Ind. Med.* 46:239–249.

Kumagai, S., and Matsunaga, I. 1995. Physiologically based pharmacokinetic model for acetone. *Occup. Environ. Med.* 52:344–352.

Kumagai, S., Oda, H., Matsunaga, I., Kosaka, H., and Akasaka, S. 1999. Uptake of ten polar organic solvents during short-term respiration. *Toxicol. Sci.* 48:255–263.

Liira, J., Riihimaki, V., and Pfaffli, P. 1988. Kinetics of methyl ethyl ketone in man: absorption, distribution and elimination in inhalation exposure. *Int. Arch. Occup. Environ. Health* 60:195–200.

McKee, R. W. 1941. Solubility of carbon disulfide vapor in body fluids and tissues. *J. Ind. Hyg. Toxicol.* 23:484.

Monster, A. C. 1979. Difference in uptake, elimination, and metabolism in exposure to trichloroethylene, 1,1,1-trichloroethane and tetrachloroethylene. *Int. Arch. Occup. Environ. Health* 42: 311–317.

Morris, J. B., and Cavanagh, D. G. 1986. Deposition of ethanol and acetone vapors in the upper respiratory tract of the rat. *Fundam. Appl. Toxicol.* 6:78–88.

Morris, J. B., and Cavanagh, D. G. 1987. Metabolism and deposition of propanol and acetone vapors in the upper respiratory tract of the hamster. *Fundam. Appl. Toxicol.* 9:34–40.

Morris, J. B. 1990. First-pass metabolism of inspired ethyl acetate in the upper respiratory tracts of the F344 rat and syrian hamster. *Toxicol. Appl. Pharmacol.* 102:331–345.

Morris, J. B., Clay, R. J., and Cavanagh, D. G. 1986. Species differences in upper respiratory tract deposition of acetone and ethanol vapors. *Fundam. Appl. Toxicol.* 7:671–680.

Morris, J. B., Hassett, D. N., and Blanchard, K. T. 1993. A physiologically based pharmacokinetic model for nasal uptake and metabolism of nonreactive vapors. *Toxicol. Appl. Pharmacol.* 123: 120–129.

Onorato, D. J., Demirozu, M. C., Breitenbucher, A., Atkins, N. D., Chediak, A. D., and Wanner, A. 1994. Airway mucosal blood flow in humans. *Am. Respir. Crit. Care Med.* 149:1132–1137.

Perbellini, L., Brugnone, F., Caretta, D., and Maranelli, G. 1985. Partition coefficients of some industrial aliphatic hydrocarbons (C5–C7) in blood and human tissues. *Br. J. Ind. Med.* 42:162–167.

Petreas, M. X., Woodlee, J., Becker, C. E., and Rappaport, S. M. 1995. Retention of styrene following controlled exposure to constant and fluctuating air concentrations. *Int. Arch. Environ. Health* 67:27–34.

Pezzagno, G., Ghittori, S., Imbriani, M., and Capodaglio, E. 1985. Urinary elimination of styrene in experimental and occupational exposure. *Scand. J. Work Environ. Health* 11:371–379.

Pezzagno, G., Imbriani, M., Ghittori, S., and Capodaglio, E. 1988. Urinary concentration, environmental concentration, and respiratory uptake of some solvents: Effect of the work load. *Am. Ind. Hyg. Assoc. J.* 49:546–552.

Ramsey, J. C., and Andersen, M. E. 1984. A physiologically based description of the inhalation pharmcokinetics of styrene in rats and humans. *Toxicol. Appl. Pharmacol.* 73:159–175.

Rosier, J., Veulemans, H., Masschelein, R., Vanhoorne, M., and Peteghem, C. V. 1987. Experimental human exposure to carbon disulfide. *Int. Arch. Occup. Environ. Health* 59:233–242.

Sato, A., and Nakajima, T. 1979a. Partition coefficients of some aromatic hydrocarbons and ketones in water, blood and oil. *Br. J. Ind. Med.* 36:231–234.

Sato, A., and Nakajima, T. 1979b. A structure-activity relationship of some chlorinated hydrocarbons. *Arch. Environ. Health* 34:69–75.

Stahl, W. R. 1967. Scaling of respiratory variables in mammals. *J. Appl. Physiol.* 22:453–460.

van Engelen, J. G. M., Haan, W. R., Opdam, J. J. G., and Mulder, G. J. 1997. Effect of coexposure to methyl ethyl ketone (MEK) on *n*-hexane toxicokinetics in human volunteers. *Toxicol. Appl. Pharmacol.* 144:385–395.

Wigaeus, E., Holm, S., and Astrand, I. 1981. Exposure to acetone. Uptake and elimination in man. *Scand. J. Work Environ. Health* 7:84–94.

Yamaoka, K. 1984. *Pharmacokinetic evaluation using micro computer,* pp. 63–69. Kyoto: Nankodo. [In Japanese]